SIXTH EUROPEAN ROTORCRAFT AND POWERED LIFT AIRCRAFT FORUM

PAPER NO. 16

DEVELOPMENT OF A BEARINGLESS HELICOPTER TAILROTOR

H. Huber
H. Frommlet
W. Buchs

Messerschmitt-Bölkow-Blohm GmbH
Munich, Germany

September 16 - 19, 1980
Bristol, England

THE UNIVERSITY, BRISTOL, BS8 1HR, ENGLAND

DEVELOPMENT OF A BEARINGLESS HELICOPTER TAILROTOR

H. Huber
H. Frommlet
W. Buchs

Messerschmitt-Bölkow-Blohm GmbH
Munich, Germany

Abstract

A composite bearingless tailrotor is currently under development at MBB, specificly designed with the objectives of improved aerodynamic efficiency, gains in simplicity, and reduction in weight and cost. The design uses a fiberglass bending-torsion-flexure to accommodate bending deflections and collective pitch control. The selection of low chordwise stiffness ("soft-inplane" concept) contributes significantly to low blade stresses, attainment of low control loads, and low weight. Main emphasis is placed upon assuring stability of the soft-inplane tailrotor, coupled with the airframe modes.

The structural design is based upon the application of advanced fiber composite materials, which provide high flexibilities, minimum stress levels, and infinite fatigue life. Two configurations, one three-bladed and one four-bladed tailrotor, are under development.

The paper concentrates on the technical design approach, and discusses detailed results of two selected systems. A major part is dealing with dynamic characteristics, aeroelastic stability, loads, and stress analyses. Results of structural fatigue and frequency survey testing of components, and of full-scale blade assemblies are presented. Expected weight and cost benefits are shortly discussed.

1. Introduction

Efforts in helicopter technology during the past decade were mainly concentrated on technical areas of mission effectiveness, ride comfort, and structural improvements. Significant steps were accomplished through advanced airfoils, improved control systems, and progress in materials, to name just a few examples. Moreover, modern helicopters of tomorrow have to be designed with greater regard also to aivailability of the aircraft for flight operations, and to commercial efficiency, in general.

There are three important areas, virtually contributing to these objectives:

(1) the reduction of production cost, through improvements in simplicity, reduction of number of parts, and modularisation of components and systems, for example

(2) the reduction of life-cycle-cost, the main emphasis being placed upon time between removal, on-condition maintenance, and reduction of maintenance hours per flight hours, for example

(3) the increase of reliability, obtainable through system simplification, and application of fail-safe philosophy.

Until recently, tailrotors have been designed with only little regard to above objectives. Tailrotors of in service helicopters were usually built as conventional systems, showing high expenditure of complex elements, such as hinges, joints, and lubricated bearings. The teetering configuration, as shown in Figure 1, is typical for many of current in service helicopter tailrotors.

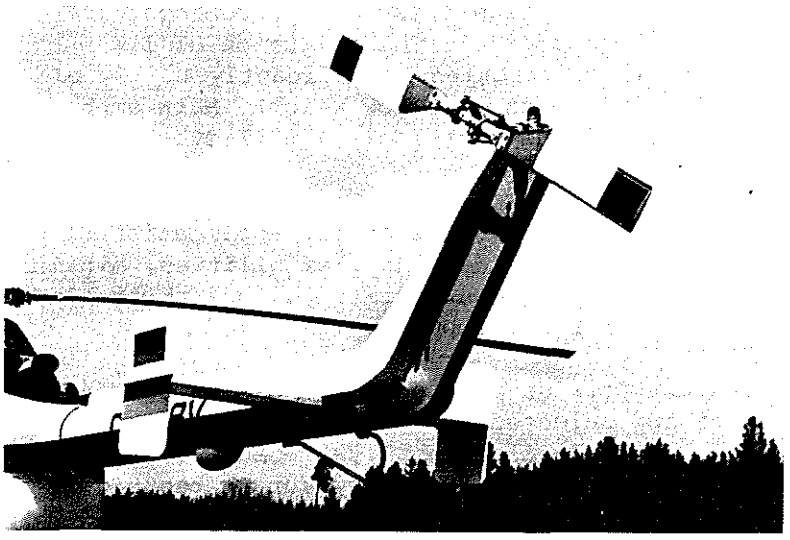

Figure 1 BO 105 Production Tailrotor

The MBB company is presently under contract with the ministry of Research and Technology of the Federal Republic of Germany to develop a composite bearingless tailrotor. Elimination of complicated mechanical elements by use of advanced fiber composite materials, showing unique combination of anisotropic properties, is one fundamental step to meet the envisaged design goal.

This paper mainly concentrates on the technical design approach, and presents and discusses detailed results of selected configurations, a three-bladed and a four-bladed system. Main emphasis is placed upon the dynamic layout, and the aeroelastic stability characteristics of the soft-inplane design. Predicted loads are presented and some results of structural stress analysis are discussed. Component tests are described, as far as they were completed till now.

2. Basic Layout Considerations

2.1 Design to Improved Performance

The general program was aimed to the development of a bearingless tailrotor with the possibility of a later use on the MBB light utility class helicopters BO 105 and BK 117. Basic aerodynamic dimensions were established under the guideline of improving thrust capability over the current production tailrotor.

The major design constraints, which had to be applied to the basic design were: Compatibility with the current tailrotor drive train, compatibility with existing pedal control system (no servo hydraulic), and being interchangeable with current tailrotor on BO 105/BK 117, with only minor modifications. Two configurations, a three-bladed and a four-bladed system were selected. Pertinent physical dimensions of new tailrotor designs, in comparison to the current production version, are presented in the following table:

Table 1 Comparison of Physical Dimensions

Item	Production Tailrotor BO 105/BK 117	Bearingless Tailrotor 3-bladed	4-bladed
Diameter, m	1.90	1.95	
Number of Blades	2	3	4
Rotor Tip Speed, m/sec	221.1/216.7	206.5	
Blade Chord, m	0.18	0.17	0.12
Rotor Solidity	0.12	0.166	0.157
Linear Twist, deg	0	-10	
Airfoil	NO012/S102E	S102C-E	
Thickness	12/8.3	12-8.3	

Major performance improvements are obtained through reduction of tip speed, advanced airfoil sections from the MBB S102-series, and twist. Comparison of thrust capabilities is shown in Figure 2.

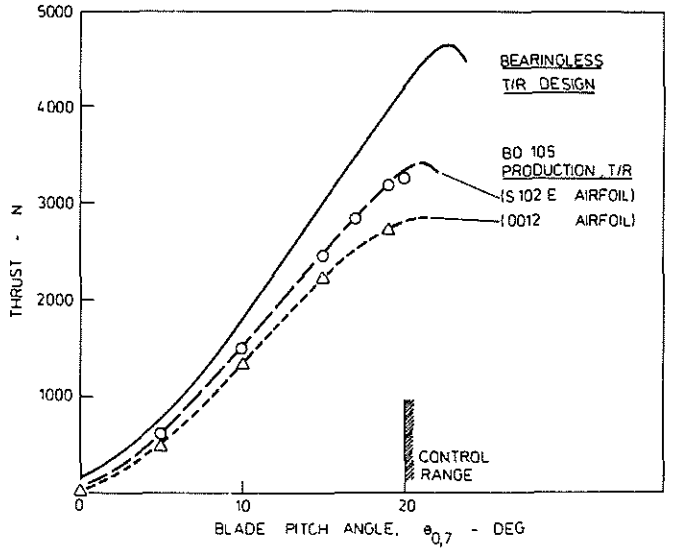

Figure 2 Improved Thrust Capability (SL. STD.)

Maximum thrust of the new design is increased by about 40%, useable maneuver thrust is about 60% higher, when compared to the existing tailrotor. Marked power reductions are obtained at increasing thrust levels and/or altitude.

2.2 Design to Reduced Noise

In view of increasing importance of noise annoyance, modern rotors have to be designed to reduced noise signature. This is especially true for tailrotors, where the cost impact is nearly negligible in case of initial designs. Classical design techniques for rotor noise reductions are well known today, and are, in general, identical to aerodynamic design requirements.

Estimates of the noise reductions, associated with the new configurations, are collected in Table 2. Reductions in hover tailrotor noise level of 3 dB(A) for the three-bladed, and of 4 dB(A) for the four-bladed concept are noted, when compared to the current production tailrotor.

Table 2 Estimated noise levels of current production and new bearingless tailrotor (rotational + broadband noise). Case: Hover flight, Thrust = 1750 N, Distance = 150 m, Height = 5 m

Type	Total Noise dB(A)
2-Bladed (production)	71.6
3-Bladed (new design)	68.6
4-Bladed (new design)	67.6

2.3 Desirable Technical Features

The primary objective of a bearingless design is freedom from lubricated bearings, fittings and joints. Obviously, the flexible part, replacing these components, is the key element of such design. The following principal technical features were considered to be of fundamental importance in the successfull development:

- Low hub moments
- Low blade stresses
- Low control forces
- High stability margins.

Frequency selection: The amount of hub moments, and of oscillating bending loads acting on the inboard portions of the blade, is governed by the fundamental frequency selection.

Comprehensive studies were conducted to determine the optimum solution in terms of chordwise frequency placement. Parametric studies have indicated that the most efficient way to reduce oscillating inplane bending is, to lower inplane frequency ("soft inplane").

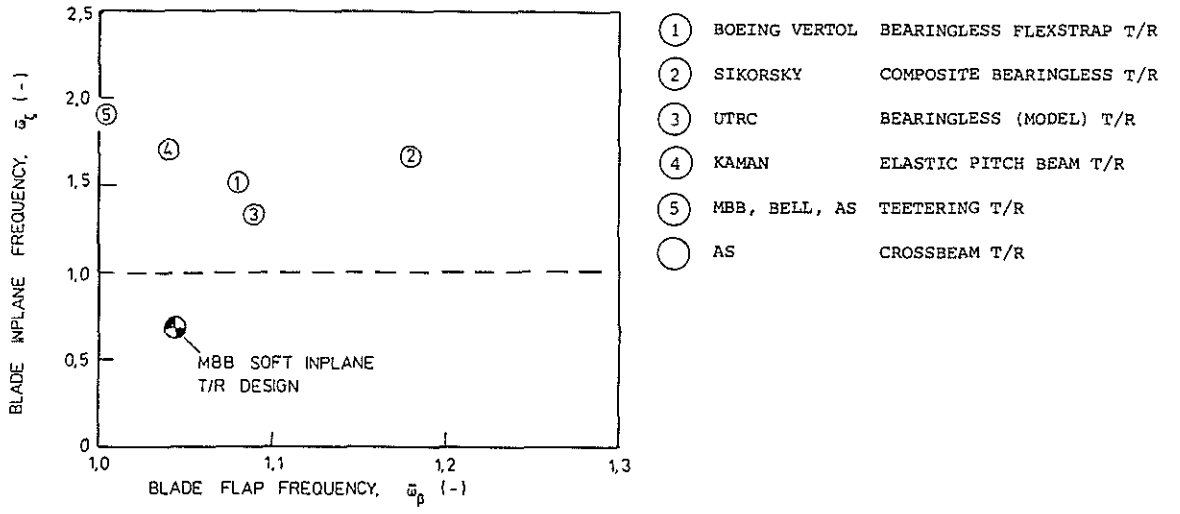

Figure 3 Characterization of Typical Tailrotor Concepts

Furthermore, low chordwise stiffness contributes significantly to attainment of low control loads, as well as to low weight. Figure 3 compares different design concepts, characterized by their fundamental flap and chord frequencies. A description of these systems is given in References 1 to 6.

Aeroelastic Stability: One stability phenomenon, which has to be resolved for soft-inplane rotor concepts, is that of lead-lag instability coupled with body motions (ground-/air resonance). The knowledge about the fundamental mechanism, and of influential parameters to provide sufficient damping, is highly developed today (References 7 to 9, for example). It became clear during the preliminary design phase, that the problem of tailrotor ground resonance can be solved by proper selection of frequencies and through adequate damping sources. The frequency diagram (Figure 4)

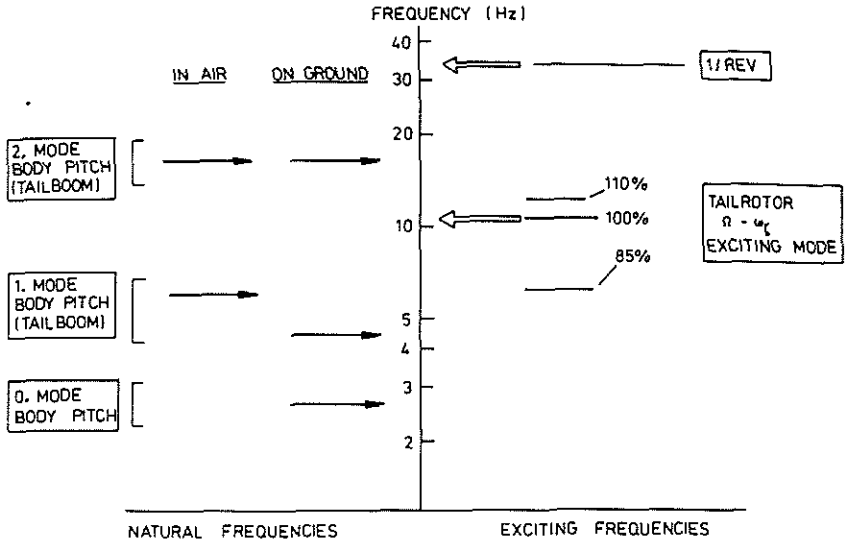

Figure 4 Fundamental Frequency Placement

indicates, that a favourable frequency window is available for the application of a soft-inplane tailrotor. A detailed analysis of the ground-/air resonance problem is given later.

Control forces: A third design constraint was, to ensure that maximum pedal forces were kept within the same level as for the standard tailrotor. The reduction of beam torsional stiffness, and the application of centrifugal counter-weights were shown to be highly effective means to meet this goal. The design requirement, that tailrotor collective pitch should be self-centering at about 6 degrees in case of a control system failure, can easily be fulfilled by tailoring mass and axis inclination of the counter-weights.

δ_3-coupling: Calculations of forward flight and maneuver conditions have indicated, that dynamic flap angles can amplify to excessive amplitudes if no feedback is used. Figure 5 shows a drastic reduction of cyclic flapping deflections with positive and negative δ_3-angles.

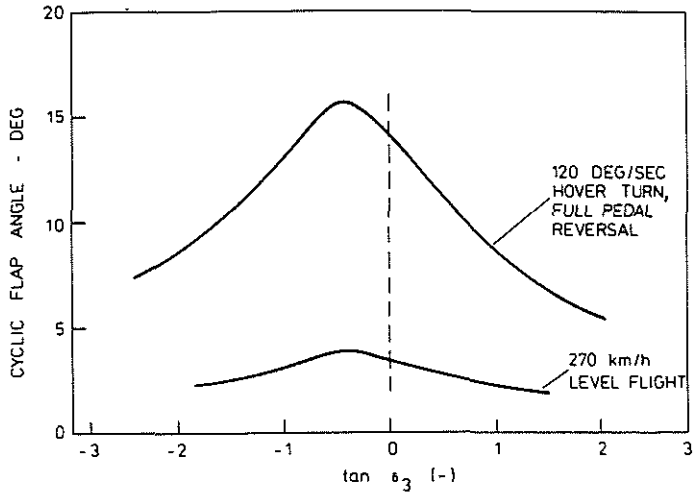

Figure 5 Cyclic Flapping as a Function of δ_3-Coupling

3. Design Description of Two Selected Systems

3.1 Components Description

Based on the stated design requirements, several variations were elaborated, differing mainly in the spar geometry, in the type of hub design, and in the pitch arm attachment, for example. Solutions were sought, which would allow both 3-bladed and 4-bladed configurations. Two typical inboard flexible element designs, which are judged to be capable of fulfilling the requirements, are shown in Figure 6.

Three bladed rotor: The fibergalss beam element is the continuation of the "C"-beam of the blade airfoil section, which converges to form two V-shape beams in the chordplane. The straps can be slotted to achieve lower chordwise stiffness, if required. Through inclination of the elements in pitch direction, it is possible, to attach the six straps to the hub by three bolts only. Bolt attachment is shifted to slightly negative

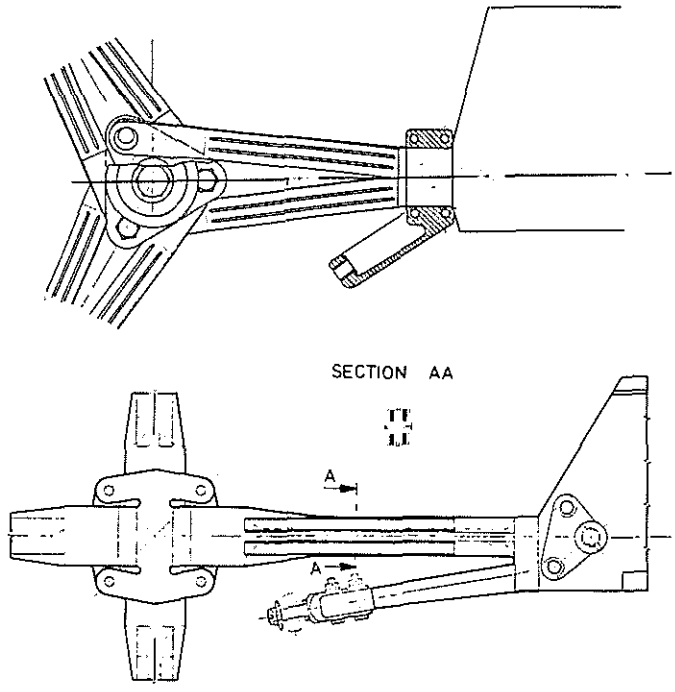

Figure 6 Flexible Element Designs;
Top: 3-Bladed; Bottom: 4-Bladed Configuration

radius, which actually keeps the flap "hinge" offset very small. The pitch horn can either be an integrated composite part, or, as shown in Figure 6, a metal part, which is fitted on the blade root by a clamp.

Four-Bladed Rotor: Basic idea was, to actually form the four-bladed system by two double-units, with the centrifugal loads of opposing blades being carried directly within the fiberglass straps. The special design of the attachment area to the hub allows low flap stiffness at the inboard region. A flat, rectangular plate, forming the "flap hinge", is continued through the pitch beam, showing a cruciform cross section. Torsional stiffness of this section is further reduced by slots, facing the shear center. On the section shown in Figure 6, an integrated damping element is applied to the chordwise flexible part, consisting of a "bridge" type construction of carbon-fiber composite plates, and viscoelastic damping material in between. The pitch-horn, which should be provided with high bending stiffness at low mass, is designed in box-beam shape with carbon-fiber composite unidirectional straps. Further design details, like material selection, section build up etc. would go beyond the scope of this paper.

On both configurations, the torsional moment counterweights will be directly attached to the blade root. By this means, the necessity of installing a separate inboard element for the transmission of the countermoment, is eliminated.

Total assemblies of the three- and four-bladed configurations are illustrated in Figure 7. It must be noted, that due to cost-reasons, the experimental rotors are manufactured, using BO 105 standard tailrotor blades (non-twisted, NACA 0012 airfoil). For the four-bladed rotor this results in an increase of solidity to about 23%, and in an increase of blade mass.

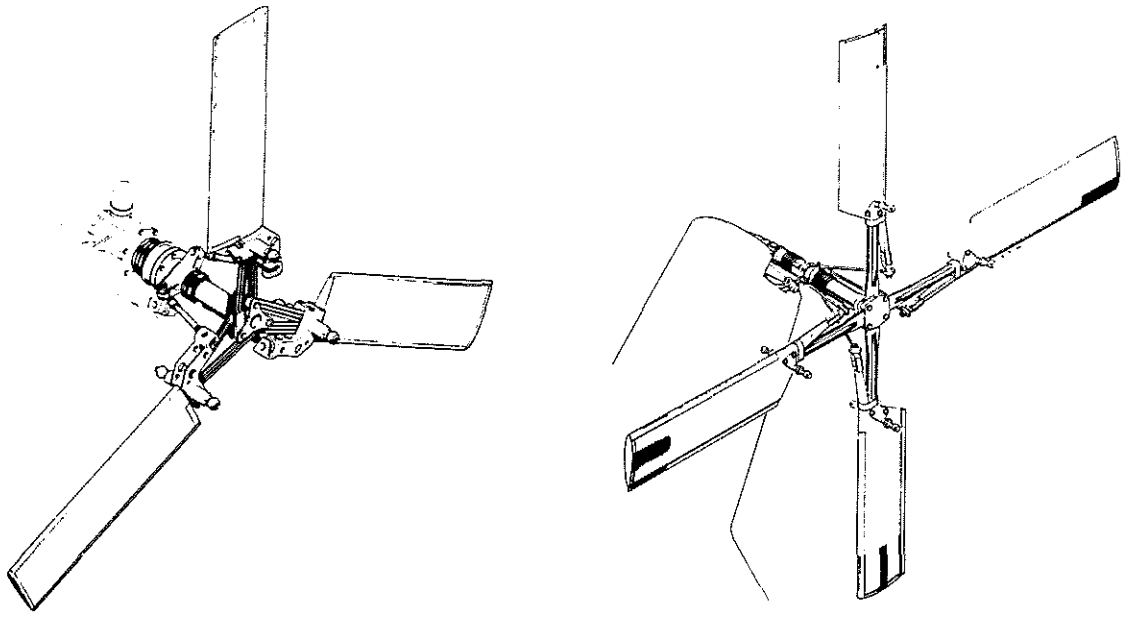

Figure 7 Tailrotor-Assemblies - 3- and 4-Bladed Configurations

3.2 Structural Properties and Dynamic Characteristics

Flap/Lag Frequencies: Basic section properties of the four-bladed system are shown in Figure 8. In flap direction, stiffness distribution is selectively tailored to concentrate flapwise curvature to a far inboard flap "hinge" at about 6 % of radius. The frequency diagram, shown in Figure 9, indicates fundamental frequencies of 1.043/rev in the flap direction, and of 0.685/rev in the chordwise direction (values at 100% rpm). With application of δ_3-coupling (+45°), the flap frequency in the air will increase to about 1.27/rev.

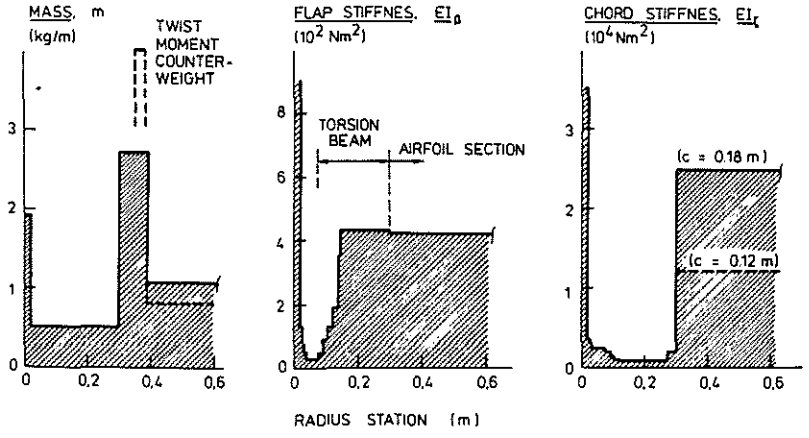

Figure 8 Section Structural Properties - 4-Bladed Configuration

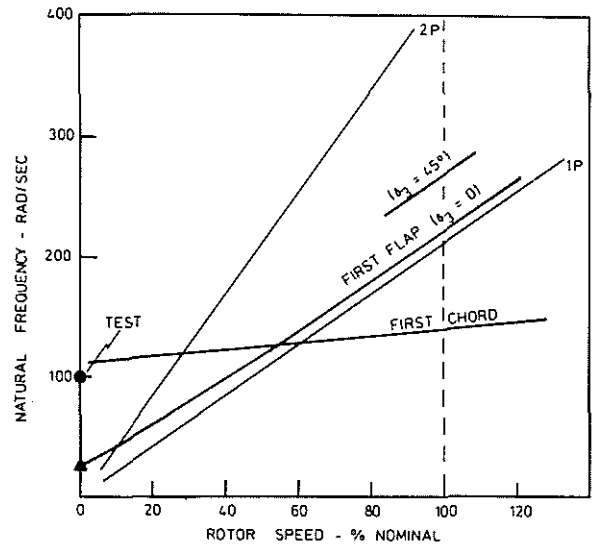

Figure 9 Fundamental Frequency Diagram - 4-Bladed Configuration

Torsional Stiffness: During bench tests, torsional stiffness was found to be as low as 0.33 Nm/deg (without centrifugal force), which can be extrapolated to a figure of ≈ 0.5 Nm/deg with centrifugal force. This value is clearly below the initial design goal (2 Nm/deg), thus drastically relieving the required twist moment compensation through counterweights. A summary of essential dynamic characteristic of both systems is presented in the following Table 3:

Tabel 3 Dynamic Characteristics

Item	3-Bladed	4-Bladed
Flap Frequency Ratio, -	1.028	1.043
Inplane Frequency Ratio, -	0.65	0.68
Equiv. Hinge Offset (Flap), %R	4.6	6.0
Equiv. Hinge Offset (Lag), %R	15.4	12.4
Torsional Stiffness, Nm/deg		0.5
Lock - Number, -	1.9	1.8
δ_3-Angle, deg	+45	+45

4. Stability Characteristics

4.1 Analytical Model

One of the major design requirements was to assure aeromechanical stability of the soft-inplane tailrotor, coupled with the body motions. For the investigation of the ground-/air resonance problem, the MBB computer program TRISTAN was used. Basic features of this model have shortly been described in Reference 7. A schematical build-up of the model is shown

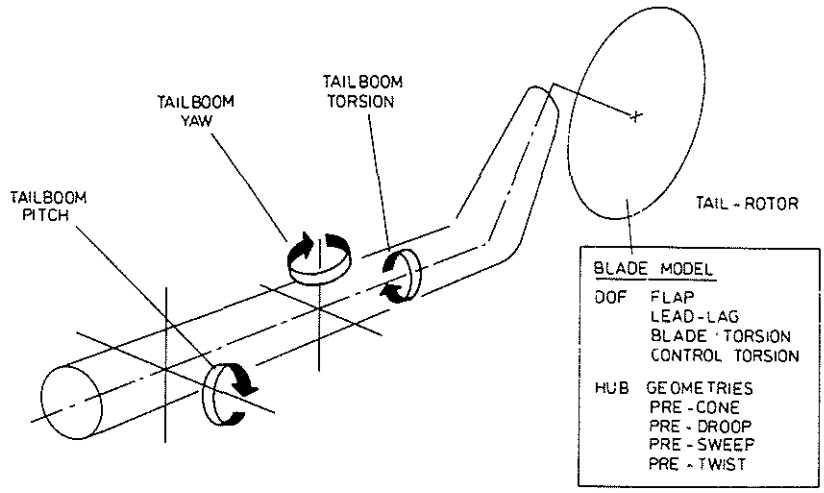

Figure 10 Coupled Tailrotor - Airframe Model

in Figure 10. It includes fully non-linear aerodynamics for hover, high speed and maneuver conditions. Elastic cantilevered blades are represented by use of the "equivalent system" technique, simulating the fundamental modes of the flap, lag, and torsional degrees of freedom. The model includes essential hub and blade geometric parameters, such as pre-cone, pre-droop, pre-sweep, and kinematic δ_1-δ_3-coupling. The airframe is represented through inertia, damping and stiffness matrices, simulating the elastic modes of the fuselage/tailboom structure.

Figure 11 presents the frequency resonance diagram for the ground-/air resonance problem. Shake tests of the BO 105 and BK 117 airframes have been conducted to obtain reliable information about the dynamic characteristics (frequencies, damping ratios) of the fuselage modes. For the helicopter on ground, pitching modes containing significant participation of the elastic tailboom, were found at 2.7 Hz, 4.4 Hz, and 16.7 Hz, with

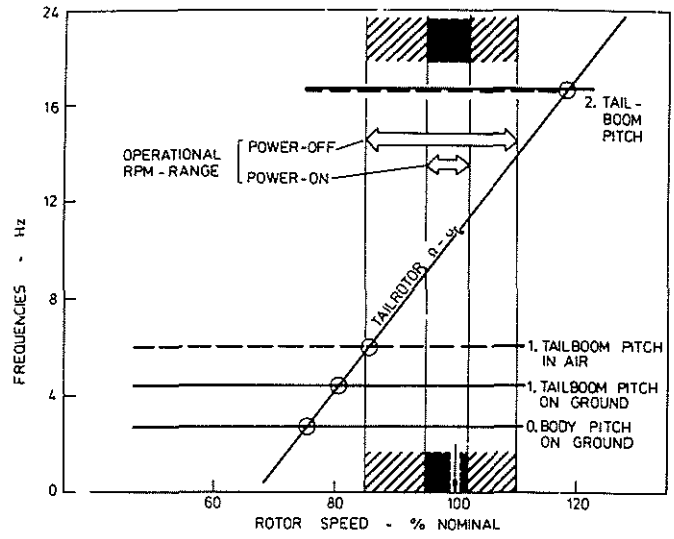

Figure 11 Ground-/Air Resonance Frequency Diagram

corresponding damping ratios between 2 and 4%. It can be seen from Figure 11, that the tailrotor exciting frequency ($\Omega-\omega_\zeta$) crosses the body pitch modes on ground at about 75 to 80%, and at 120% rotor speed. Coalescence of $\Omega-\omega_\zeta$ with the tailboom pitch mode in the air is noted at about 85% rotor speed.

4.2 Stability Results

Ground resonance stability results of the 4-bladed tailrotor configuration are shown in Figure 12. The figure illustrates damping versus rotor speed for zero thrust. With structural damping of 2 percent (tail-

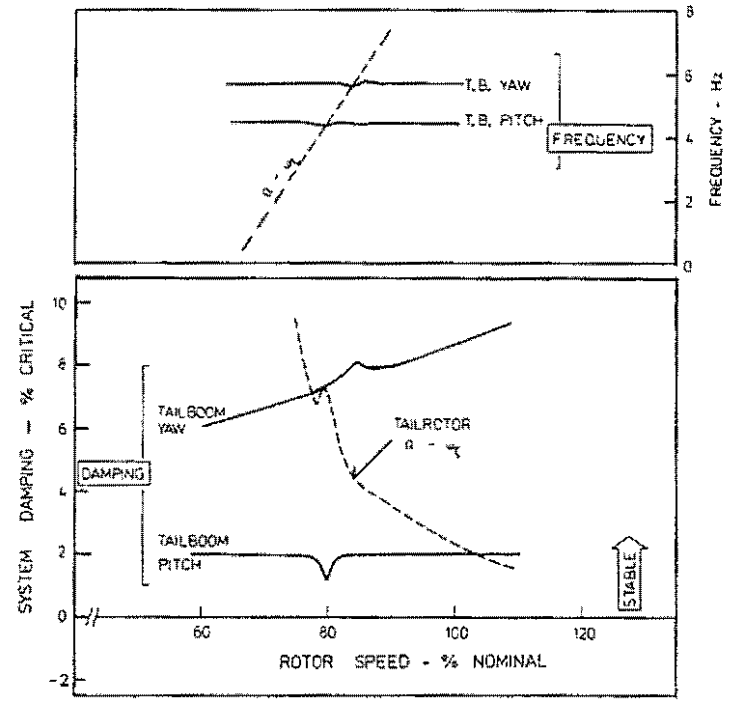

Figure 12 Ground-Resonance Mode Damping vs. Tailrotor Speed, 4-Bladed Configuration, Zero Thrust

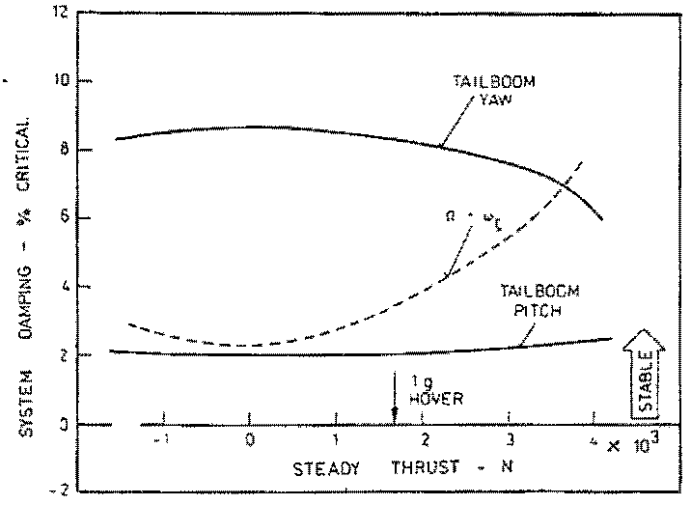

Figure 13 Ground-Resonance Mode Damping vs. Tailrotor Thrust, 4-Bladed Configuration, 100% Rotor Speed

boom vertical motion) and of 1 percent (rotating blade), damping is positive over the whole rotor speed range. Minimum damping of about 1.2% is obtained at the resonance point. Tailboom lateral damping is seen to increase to about 8 %, due to high tailrotor inflow damping.

Typical damping variation with tailrotor thrust is shown in Figure 13. At hover thrust level, damping of 2% for the tailboom pitch mode, and of 3.5% for the $\Omega-\omega_\zeta$ mode is predicted. The reduction of the tailboom lateral damping at very high thrust levels is due to blade stall effects at the blade tip.

Comprehensive stability investigations were also conducted for the resonance conditions in the air. As was noted before (Figure 11), the fuselage/tailboom pitch mode frequency in air is at about 6 Hz, and the tailboom lateral/torsional mode at about 7 Hz. Coalescence of these frequencies with the lead-lag regressing mode frequency occurs at rotor speeds just at the lower limit for power-off conditions. Results of airresonance analysis have indicated that even for the most critical condition (tailrotor thrust zero), adequate stability margin exists. The tailboom lateral/torsional mode shows damping ratios in excess of 10% critial.

4.3 Parametric Influences

During the design phase, the analytical model was very helpful in providing insight into parametric stability influences. In particular, variations of inplane frequency, δ_3-coupling, inclination of the torsional element, and of blade structural damping were investigated.

The effect of blade damping on stability is seen from Figure 14. Note, that the $\Omega-\omega_\zeta$ mode becomes unstable between one and zero percent of blade damping. Based on the existing resonance and damping conditions of the fuselage, a value of about 1.5 percent inplane damping of the rotating blade is considered to be necessary for assuring aeromechanical stability under all critical conditions.

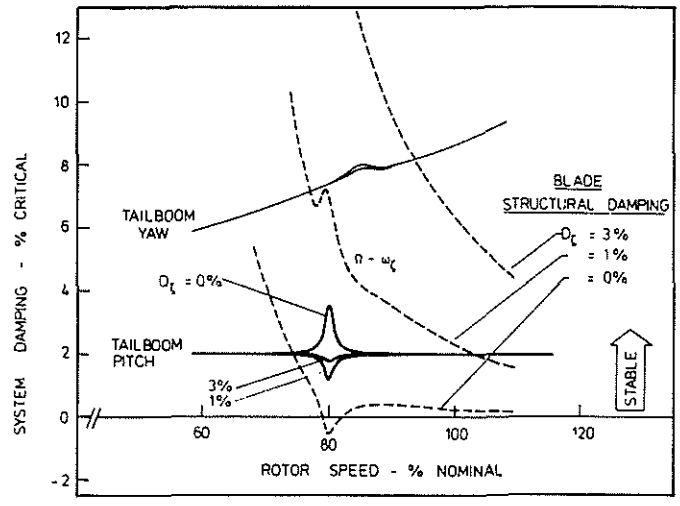

Figure 14 Effect of Blade Lead-Lag Damping on Ground-Resonance Damping, Zero Thrust

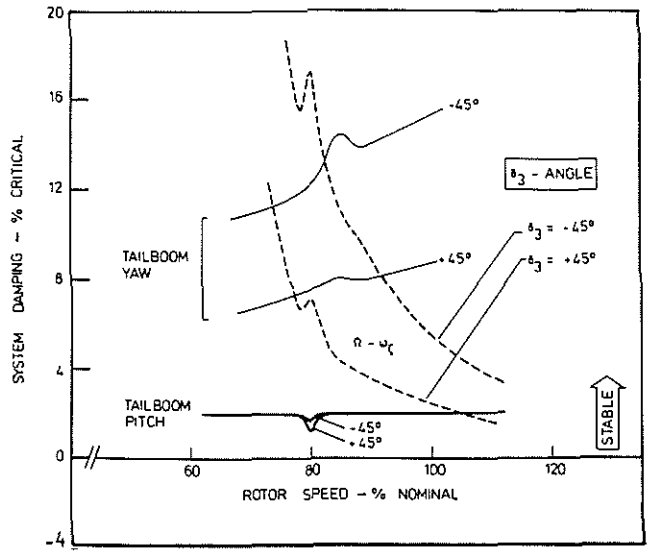

Figure 15 Effect of δ_3-Angle on Ground-Resonance Damping, Zero Thrust

Figure 15 shows the effect of δ_3-angle on the tailboom - tailrotor aeromechanical stability on ground. Negative δ_3 (i.e. flap up - pitch up) is highly stabilizing. The influence of the sign of δ_3-coupling on damping will be experimentally investigated during whirl tests. Change of sign of δ_3 can easily be done on the three-bladed configuration by reverse mounting of the pitch-horn assembly .

A technology program is conducted, to evaluate methods for increasing blade inplane damping. Figure 16 shows results of laboratory damping tests, using viscoelastic damping elements, bonded to fiberglass test specimen. Damping ratio is seen to increase from a about 1% for the non-treated element to about 3 to 5% critical for the element with damper.

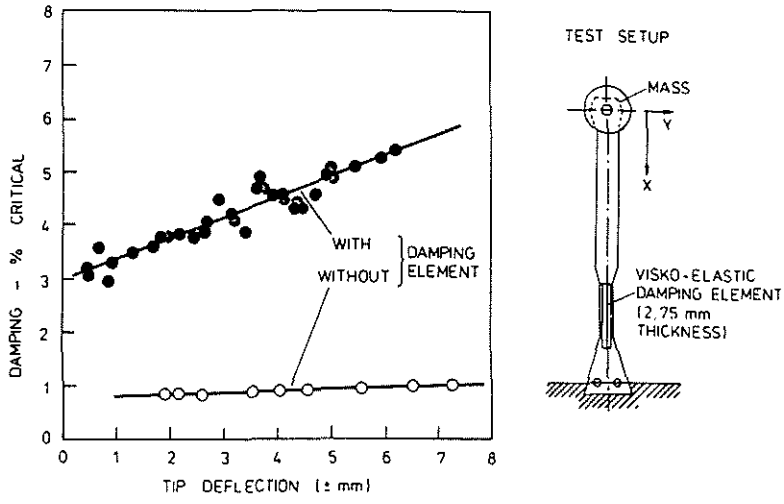

Figure 16 Laboratory Test Results of Integrated Viscoelastic Damping Element

For final application, damping elements are under development which will be bonded to the torsion beam structure, as it is illustrated in Figure 6. The integrated damping element consists of 4 damping sheets, bridged by a stiff carbon-fiber composite strap. The elements are bonded to each of the four flat plate parts of the cruciform section (four-bladed rotor).

5. Loads and Structural Analysis

5.1 Loads Prediction

The analytical model, used for load predictions, is calculating elastic blade deflections, shear forces, and bending moments at the inboard blade/hub stations, as well as control loads. Bending loads distributions at the more outboard stations are derived via corresponding moment and shear force distributions, as obtained from a mode shape analysis.

Flight conditions considered to be most critical for tailrotor loads are:

- Maximum level flight speed
- V_D-speed under 5 deg sideslip angle
- Hover turns, with pedal reversal
- 1/rev gravitational excitation during run up.

Cyclic flapping angles, vibratory flap and chordwise bending moments, and hub moments were calculated for the different flight conditions. Figure 17 presents a summary of typical flapping angles and corresponding hub moments acting on the tailrotor shaft. Highest values are calculated for an ultimate flight condition of a 120 degrees per second right turn, with a sudden full left pedal reversal applied.

In Figure 18, typical steady and vibratory bending moments in the flap and chord direction are drawn vs. blade radius. Note, that the torsional elastic beam is widely deloaded from bending moments. In the far inboard region,increasing flap and inplane bending moments are superposed to the centrifugal force.

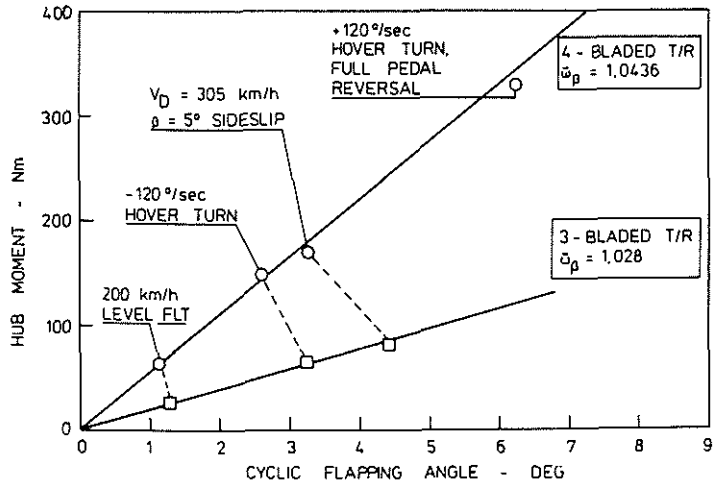

Figure 17 Hub Moments vs. Cyclic Flapping

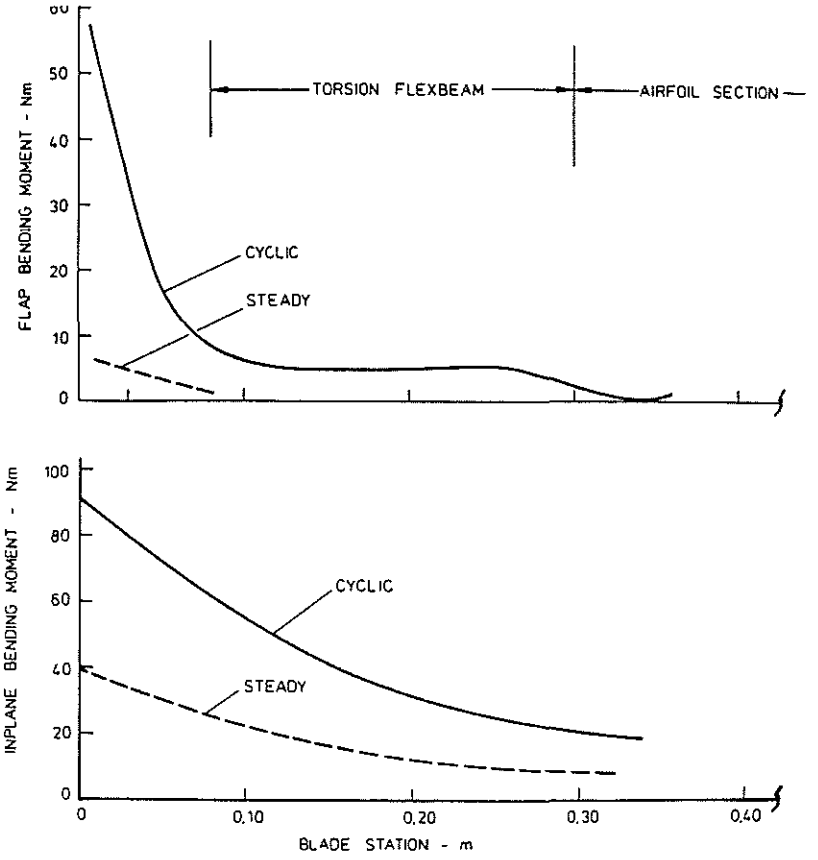

Figure 18 Flap and Inplane Bending Moment Distribution vs. Span, V_D = 305 km/h, 5° Sideslip

Total control load is influenced by the elastic twist moment, by inertia moments of blades and of counterweights, and by the aerodynamic moment. Figure 19 shows calculated control forces in the fixed system. Only small counterweights are necessary, to obtain an equivalent pedal force slope as on the two-bladed BO 105 production tailrotor. Highest osicllatory control loads of ± 480 N (rotating pitch link) were calculated for the flight case of full pedal reversal during a 120 degrees per second right turn.

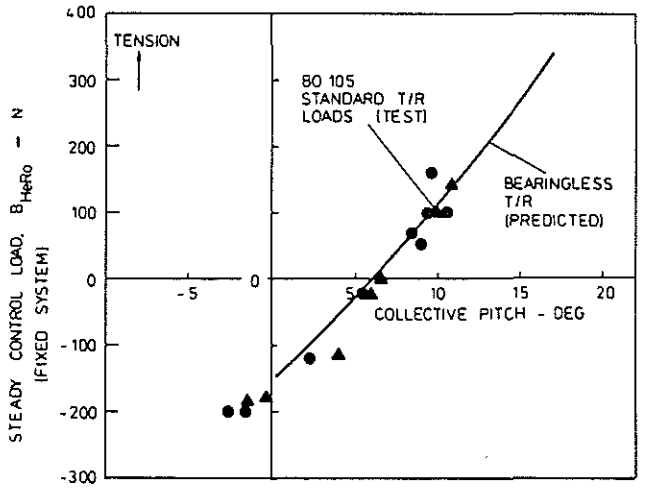

Figure 19 Calculated Control Loads, Compared to Standard Tailrotor Forces

5.2 Structural Analysis

During the detailed design phase, different analytical methods were used to determine the effective stresses of the key design elements. A finite element model was used to investigate the torsional elastic element, which is mainly loaded by shear stresses, due to maximum torsion of 14 degrees. The idealized cross-section is shown in Figure 20.

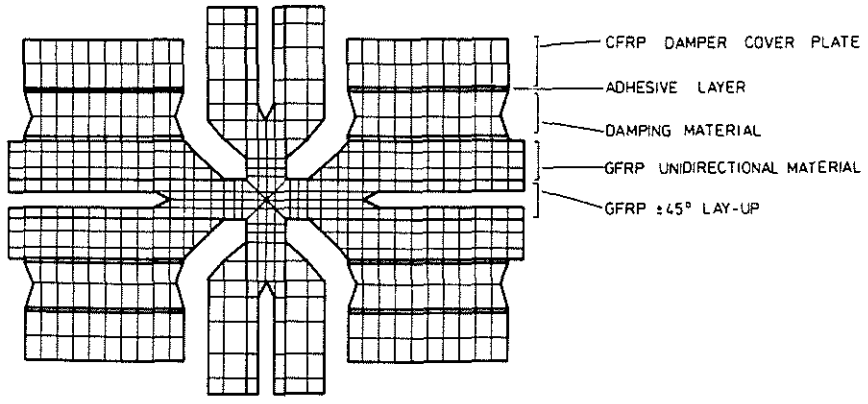

Figure 20 Idealization of Flexbeam Cross Section - 4-Bladed Configuration

For the inner parts of the blade attachment area, the more interesting load cases are combined loadings caused by centrifugal force and the two directions' bending moments. Figure 21 illustrates the relative load contributions to the maximum stress level, as a function of radius. This figure indicates, that, at far inboard stations, centrifugal force and oscillating flap bending moments account for a comparatively high portion of the total tensile stress.

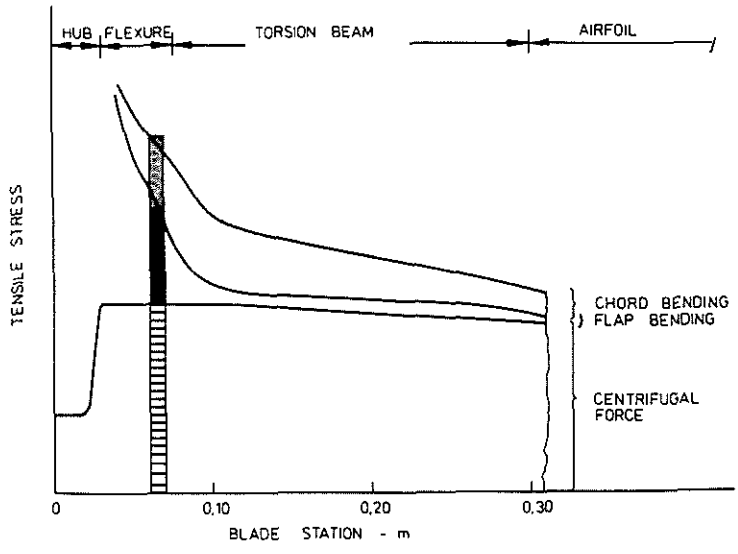

Figure 21 Predicted Tensile Stress Distribution, High Loading Case

6. Components Testing

Several component tests were conducted, to confirm stress analyses and, finally, to reduce development risk. Different test samples in full-scale hardware were fabricated, strain gaged, and tested. A flap flexure element (test mounting see Figure 22) was loaded by a 25 kN steady centrifugal force, and by oscillating flap bending loads. During 10^7 cycles, a maximum strain of $7.7^{o}/oo$ was recorded, without any structural damage. Bench tests were also conducted to simulate steady and dynamic torque moments, and maximum oscillating inplane moments of ± 140 Nm. During 10^6 cycles, maximum tensile strain of $3.7^{o}/oo$ was observed.

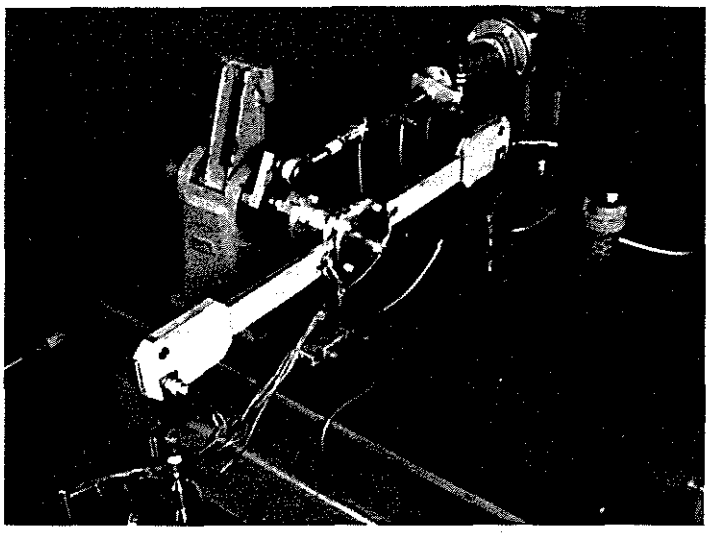

Figure 22 Laboratory Mounting of Flap Flexure Element for Centrifugal-Bending Tests

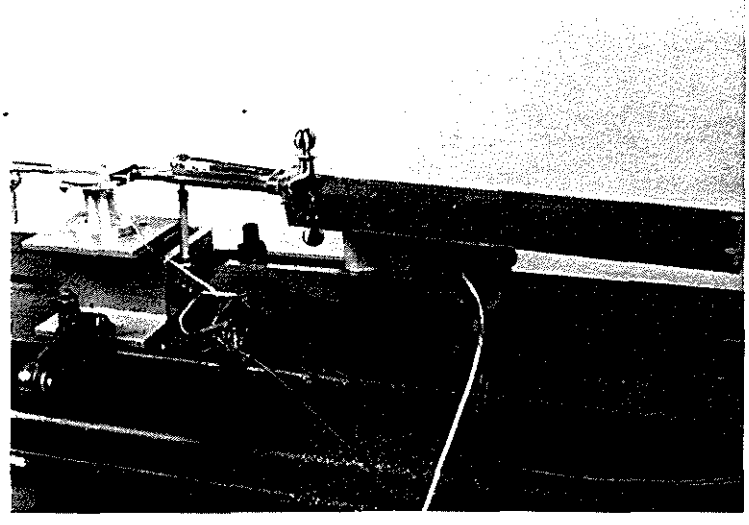

Figure 23 Laboratory Setup for Nonrotating Frequency/Damping Tests

Frequency survey testing, including determination of damping characteristics (Figure 23), and structural fatique testing of a complete flexure/blade assembly are presently performed. Time variations and phase relationships of shear forces, bending moments, cyclic blade deflections, and steady and cyclic beam twist are applied, which were derived from the analytical simulation results.

7. Manufacturing of Hardware

Manufacturing of whirl-tower and experimental flight test hardware had to be conducted under reduced costs. It, therefore, was decided to apply the airfoil section of the current production tailrotor blade. This section is differing from the new design, as noted in chapter 3.1. Two standard blade moulds are attached to the new center mould of the flexbeam and hub attachment section. Two opposite blades are fabricated in a double-unit, the carrying fibers going directly from one blade to the other, through the hub.

Figure 24 shows full scale hardware of the three- and four-bladed configuration, ready for assembly with metal bracket parts.

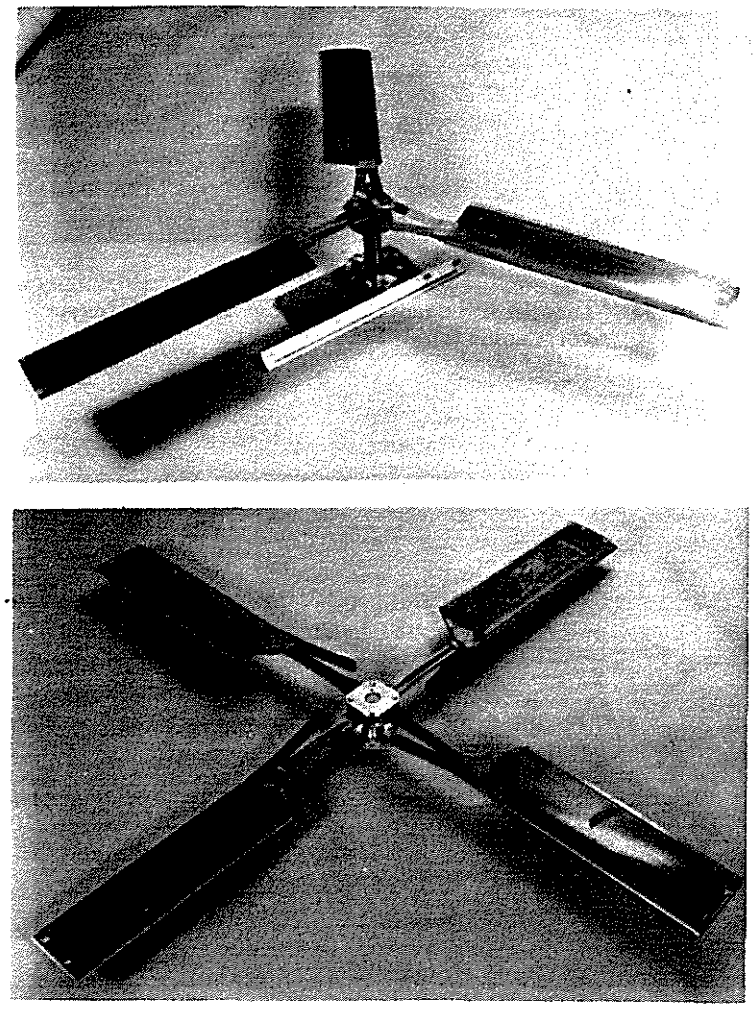

Figure 24 Full-Scale Tailrotors - 3-Bladed, and 4-Bladed Configuration

8. Weight and Cost Estimates

Turning back to the initially stated objectives of this development program, the judgement of improvements and merits of the new designs is of great intrest. When relating the component weight to equivalent performance capabilities, a weight reduction of about 20% is assigned to the new configurations, comparing to 12 kg basic weight of the conventional tailrotor with the same thrust capacity.

What the question of cost is concerned, production cost of the composite material parts of the new designs are only slightly higher than that of the fiber parts (i.e. blades) of the conventional system. However, metal parts cost are fairly reduced, so that procurement cost savings of the amount of 20% are estimated.

Finally, due to on-conditions maintenance qualities, and infinite life of all components, significant service cost savings will be realized by the new designs.

9. Next Program Phases

Next test activities of complete tailrotor assemblies will involve full-scale whirl testing of the three- and four-bladed versions. Major goals of this test program will be to establish blade dynamic characteristics (i.e., rotating frequencies, lead-lag damping), control loads, blade deflections, and stress data. For simulating dynamic loads on ground, the whirl stand will be equipped with a precession capability, with maximum yaw rates of ± 120 degrees per second. The basic build up of the test-stand is designed to serve both as a stiff support, and as a mass-spring-damper system, representing tailboom dynamics. The control system is designed to allow dynamic control inputs, to provide excitation of the different rotor modes.

After completion of full-scale whirl tests, the tailrotor prototypes will be flight tested on a BO 105 helicopter. At least one of the two configurations will then be selected, updated, and prepared for final flight qualification.

10. Conclusions

Based on the existing development status, the following conclusions can be drawn:

- Basic aerodynamic layout of the new tailrotor design will result in significant performance improvement, and reduction in noise, when comparing to the current production version.

- Two different configurations - three-bladed and four-bladed - have been selected for further detailed design and testing. Structural designs are based upon the extensive use of appropriate fiber composite material.

- In particular, the selection of low chordwise stiffness ("soft-inplane" concept) contributes significantly to low vibratory bending loads, low control loads, and low weight.

- Aeromechanical stability (ground-/air resonance mode) of the soft-in-plane solution can be ensured by proper frequency selection, and adequate blade damping. Predicted stability margins require further test proving. Methods for providing additional blade damping on the basis of integrated elastomeric elements are currently evaluated.

- Through low torsional stiffness of the flexible element and by application of fixed counterweights, pedal control forces can be kept within the same level as for the two-bladed production tailrotor, i.e. the new tailrotor can be flown without servo hydraulic.

- A weight and cost reduction in the range of 20% can be achieved, when comparing the new designed bearingless tailrotors to the conventional tailrotor with the same thrust capacity.

11. References

1. J. Shaw, W.T. Edwards — The YUH-61A Tailrotor: Development of a Stiff Inplane Bearingless Flexstrap Design, 33rd Annual National Forum of the American Helicopter Society, Preprint No. 77.33-32, May 1977

2. R.R. Fenaughty, W.L. Noehren — Composite Bearingless Tailrotor for UTTAS, 32nd Annual National V/STOL Forum of the American Helicopter Society, Preprint No. 1084, May 1976

3. R.L. Bielawa — Aeroelastic Characteristics of Composite Bearingless Rotor Blades, 32nd Annual National Forum of the American Helicopter Society, Preprint No. 1032, May 1976

4. J.D. Porterfield, F.B. Clark — Elastic Pitch Beam Tailrotor for LOH, Kaman Aerospace Corporation, USAAMRDL TR 75-41, Fort Eustis, VA, Juli 1976

5. K.W. Harvey, Ch.W. Hughes — Design, Analysis, and Testing of a New Generation Tailrotor, 35th Annual National Forum of the American Helicopter Society, Preprint No. 79-57, May 1979

6. R. Mouille — Ten Years of Aerospatiale Experience with the Fenestron and Conventional Tailrotor, 35th Annual National Forum of the American Helicopter Society, Preprint No. 79-58, May 1979

7. H.B. Huber — Effect of Torsion-Flap-Lag Coupling on Hingeless Rotor Stability, 29th Annual National Forum of the American Helicopter Society, Preprint No. 731, May 1973

8. R.A. Ormiston — Concepts for Improving Hingeless Rotor Stability, American Helicopter Society Symposium on Rotor Technology, Essington, Pa., August 1976

9. D.H. Hodges — An Aeromechanical Analysis for Bearingless Rotor Helicopters, 34th Annual National Forum of the American Helicopter Society, Paper No. 78-21, May 1978